BUILDING TRAINING PATTERNS FOR MODELLING *MR* DAMPERS

Jorge de-J. Lozoya-Santos, Javier A. Ruiz-Cabrera, Vicente Diaz-Salas
Ruben Morales-Menendez and Ricardo Ramirez-Mendoza
Tecnológico de Monterrey, Av. Garza Sada 2501, Monterrey, NL, México

Keywords: Pattern validation, Modelling, Magneto-rheological damper, Identification.

Abstract: A method for training patterns validation for modelling *MR* damper is proposed. The method was validated with two models based on black-box and semi-phenomenological approaches. An input pattern that allows a better identification of the *MR* damper model was found. Including a frequency modulated displacement and increased clock period in the training pattern, the *MR* damper model fitting is improved. Also, the designed input pattern minimizes of training phase and reduces of the number of experiments. Additionally, incorporation of the electric current in the *MR* models outperforms the modelling approach.

1 INTRODUCTION

A Magneto-Rheological (*MR*) damper is a device which allows the dissipation of energy in a automotive suspension. Its principal components are: piston, housing, accumulator, coil and *MR* fluid. The mechanical structure is the unchanged of passive damper. The *MR* fluid is a suspension of micrometer-sized magnetic particles in an oil. In the area of piston where the oil is transfered between housing chambers, a magnetic field is applied via electric current. The later varies the damping properties of the device. The interaction of the several aforementioned mechanisms and the magnetic field variations results in highly non linear behavior with hysteretic patterns of the generated force.

The power generated and energy dissipated by this device are defined by the piston displacement and velocity multiplied for the force, respectively. In the control system of a semi-active automotive suspension, the precision on the generated power and dissipated energy of *MR* damper is crucial. This precision depends on the accuracy of the *MR* damper model. Therefore, a good *MR* damper model is a key issue. Having a good *MR* damper simulation demands a good mathematical equation of the damper, a good training phase and a good learning phase of the model (coefficients). The training phase must find out the main characteristics of the *MR* damper through the training patterns. This requires a specific Design of Experiments (*DoE*).

The role that the input patterns plays in the *MR* damper identification process was analyzed with two models. The hypothesis is that there exists experimental input patterns that allows the best learning of the coefficients of the model, regardless the chosen model structure. This paper is organized as follows. Section 2 presents a literature review. In section 3, several input patterns were implemented in order to validate the proposal. Section 4 discusses the results. Section 5 concludes the paper.

2 LITERATURE REVIEW

2.1 Input Patterns

The training patterns of the most representative modeling approaches were reviewed. In some research works the Design of Experiments (*DoE*) and the *MR* damper model were not clearly associated. The development of a *MR* damper model, its parameterization and its final application were not integrally performed.

A training pattern for modelling of a *MR* damper consists of signal that includes a displacement (x) and electric current (I). The velocity is considered as a rate of change of the displacement. Table 1 summarizes some important works. This table is divided in three sections according to the training patterns.

Section one (SSS+C). The displacement is a

de-J. Lozoya-Santos J., Morales-Menendez R., A. Ruiz-Cabrera J., Diaz-Salas V. and Ramirez-Mendoza R. (2009).
BUILDING TRAINING PATTERNS FOR MODELLING MR DAMPERS.
In *Proceedings of the 6th International Conference on Informatics in Control, Automation and Robotics - Signal Processing, Systems Modeling and Control*, pages 156-161
DOI: 10.5220/0002215501560161

Table 1: Comparison of *MR* damper models. *P*ower column shows if the research work studied the generated power (✓), or did not (✗). *E*nergy column same meaning as power column. Finally, the reference are cited.

Power	Energy	SSS+C training patterns
✓	✓	(Spencer et al., 1996)
✓	✓	(Li et al., 2000)
✓	✗	(Wang and Kamath, 2006)
✗	✗	(Shivaram and Gangadharan, 2007)
✓	✓	(Guo et al., 2006)
✓	✓	(Nino-Juarez et al., 2008)
Power	Energy	BWN+C training patterns
✗	✓	(Burton et al., 1996)
✗	✗	(Wang and Liao, 2001)
✗	✗	(Savaresi et al., 2005)
Power	Energy	BWN+BWN training patterns
✗	✗	(Wang and Liao, 2001)
✗	✗	(Chang and Zhou, 2002)
✓	✓	(Du et al., 2006)

*S*inusoidal *S*weep *S*ignal (*SSS*) with specific frequency and a *C*onstant electric current. This is a typical training input for *MR* damper models. Exploiting this pattern, both *E*nergy (*E*) and *P*ower (*P*) are successfully simulated. The number of experiments is high. The obtained model accuracy is high (5% error). There are not electrical current transients, this compromises the use of the model. Table 1 shows six representative works with this type of training inputs.

Section two (BWN+C). The displacement is a bandwidth *B*and*W*idth *N*oise (*BWN*) pattern and a *C*onstant electric current (*C*). This training input patterns has the same features as SSS+C signals. However, the information richness due to the magnitude of displacement is decreased. *P*ower and *E*nergy simulation are not achieved.

Section three (BWN+BWN), both displacement and electric current follow a bandwidth noise *BWN* pattern. Power and energy simulation are not achieved, except if a displacement greater than 10 mm is generated, (Du et al., 2006). The pattern requires shorter training inputs. The fitting error this pattern is low (3%).

The *B*and*W*idth (*BW*) in all the reviewed works was lower than 6 Hz, except in (Savaresi et al., 2005) and (Nino-Juarez et al., 2008). Hence, the *MR* damper response to high frequency has not been explored. Neither, hard non-linearities due to the broken magnetic bounds of metallic particles (because of high frequency and displacements). There are missing analysis of power and energy responses in automotive applications for frequencies around 10-15 Hz and displacement greater than 10 mm.

There are research works with other type of patterns, such as, *A*mplitude *P*seudo *R*andom *B*inary *S*ignal *APRBS* in electric current (Savaresi et al., 2005). (Wang and Liao, 2005). explored electric current with sinusoidal wave signals.

There are not a standard definition of training patterns in order to identify the power and energy features. The overuse of the *MR* damper due to long experimental exploration at electric current greater than 3 amperes could give a skewed model. Therefore, more research of training patterns for *MR* damper modelling is needed.

2.2 Modeling Approaches

Several models have been developed with different approaches. These models could be: phenomenological (*P*), semi-phenomenological (*SP*) and black-box (*BB*) (neural network, fuzzy, non-linear ARX, polynomial among others). The training pattern will be tested with both non-linear with *A*uto *R*egressive e*X*ogenous inputs (*NARX*) and a *S*emi-*P*henomenological models. A brief review of these models will be included for completeness.

Table 2: Description of variables for DoE.

Variable	Description
x_k or x	Damper piston displacement
I_k or I	Electrical current
$\dot{x}_k$ or $\dot{x}$	Damper piston velocity
f_{MRk} or f_{MR}	Damping force
a_j	j-esime modeling coefficient
d	time delays
q_1, q_2	Electrical current exponents
ESR	Error-Signal-to-noise Ratio
k	Discrete sample, discrete time
j	Subindex

The *MR* damper model based on a non-linear ARX structure is a lineal combination of a vector of delayed inputs multiplied for their parameters. If electric current is not an input, all the parameters have a polynomial dependence on it.

In (Nino-Juarez et al., 2008), a non-linear ARX model of nine parameters (1) achieves high precision simulation of power and energy. Table 2 defines the parameters of this equation.

$$\begin{aligned} f_{MRk} &= a_1 f_{MRk-1} + a_2 f_{MRk-2} + a_3 f_{MRk-3} \\ &\quad + a_4 x_{k-1} + a_5 x_{k-2} + a_6 x_{k-3} \\ &\quad + a_7 \dot{x}_{k-1} + a_8 \dot{x}_{k-2} + a_9 \dot{x}_{k-3} \end{aligned} \quad (1)$$

By the side of Semi-Phenomenological (*SP*) approaches, the bi-viscous and hysteretic behavior are shaped with smooth and concise forms. The instantaneous force is delivered without taking into account

the transients, and consequently at high frequency, dynamic features are not well emulated. Transients can be omitted at both low frequencies and small displacements. The coefficients are related to energy and power features of *MR* dampers but they are not linked to components. The SP model has a good balance between simulation capability and easy to fit model.

(Guo et al., 2006) (2) have well defined parameters for the dynamic yield force, the post-yield and the pre-yield proportions. The the *MR* damper response is simulated using hyperbolic tangents.

$$f_{MR} = a_1 tanh\left(a_3\left(\dot{x} + \frac{a_4}{a_5}x\right)\right) + a_2\left(\dot{x} + \frac{a_4}{a_5}x\right) \quad (2)$$

The non-linear ARX model has less than 1% error prediction; while the SP approach has less than 4% error prediction.

3 EXPERIMENTS

The specimen tested was a DELPHI Gabriel *MR* damper. It is a standard mono-tube configuration with 36 mm piston and *MR* fluid. This damper is part of the Delphi MagneRide^{TM} commercial system. The configuration of the experimental system was a MTS^{TM} which can deliver enough force and time response with respect to the maximum force and bandwidth of the *MR* damper.

The monitored variables were the damping force f_{MR}, displacement x, and electric current I. The data acquisition system was Software Testlink^{TM} and Testware^{TM} II). Thanks to *Metalsa*[1] for using its facility.

The DoE considered a displacement that follows this signal $0.0125 \cdot sin(\omega \cdot \frac{k}{512})$, where the sampling frequency was 512Hz, $\omega = 2\pi f$, $f = \{1, 1.5, \ldots, 13.5, 14\}$ Hz. The absolute resultant range for the displacement was $[0, 25]$ mm. The absolute resultant range for the force was $(0, 2.850]$ N. The current was kept constant.

The displacement signal was replicated 12 times. At each replicate, the current was increased in 0.25 A from 0 to 4 A. Figure 1 shows an example of these experimental results.

All the experimental data sets were identified with a semi-phenomenological model obtaining a *MR* damper simulator (Guo et al., 2006).

In order to generate several datasets, eleven training patterns were designed. The Table 3 shows two example of this. The displacement follows a

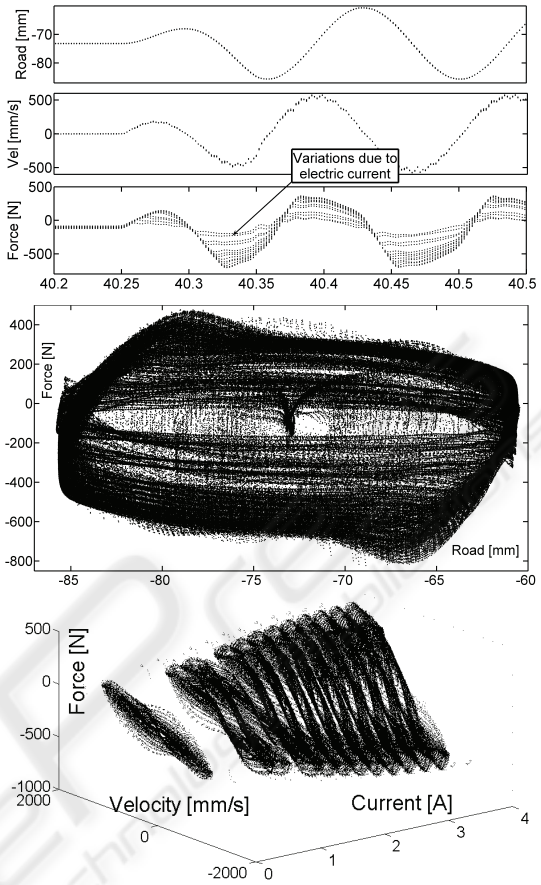

Figure 1: Experimental data for $4.5 - 14.5$ Hz (high frequency). Top plot. Time versus displacement, velocity and force response. Middle and bottom plots show the experimental energy and power. These plots include several force responses according to applied electric currents.

*F*requency *M*odulated *FM* signal with fixed amplitude and a *BW* from 0.5 to 14.5 Hz. This signal was generated by a Voltage Controlled Oscillator (*VCO*). The *VCO*'s input was an *ICPS* with values between 0 and 1. Each ICPS step had a time length of 100*ms* which means that the frequencies in signal were constant over same time. The magnitude of displacement was held constant in 3 mm. Two different signals of electric current were evaluated: an *I*ncreased *C*lock *P*eriod *S*ignal (*ICPS*) and a *P*seudo *R*andom *B*inary *S*equel (*PRBS*). The length of time was 30 seconds. All the experiments were piecewise designed, assuring the invariance of conditions during all the experiment. The signals were fed through the simulator in order to retrieve the force.

For the displacement, the several DoE forms were: *S*inusoidal *S*tepped *F*requency (*SFS*), *S*inusoidal *CH*irp Signal (*CHS*), *R*oad *P*rofile (*RP*) and (*FM*).

For the electric current, the DoE shapes were:

[1] www.metalsa.com.mx

*S*tepped increment at electrical *C*urrent (*SC*), *R*amp Periodic positive slope *C*urrent (*RC*), *R*amp with positive and negative slope *C*urrent (*ADRC*), *ICPS*, and *PRBS*.

With later defined signals the DoEs were:(1) (SFS,SC), (2)(SFS,RC), (3)(SFS,ADRC), (4)(CHS,ICPS), (5)(CHS,PRBS), (6)(SFS,ICPS), (7)(SFS,PRBS), (8)(FM,ICPS), (9)(FM,PRBS), (10)(RP,ICPS) and, (11)(RP,PRBS). The precedent number will identified the training patterns in the rest of the paper. For rich details, see (Lozoya-Santos et al., 2009).

Table 3: Design of experiments.

PTIC	Displacement $\tau(vco)$ *Time*	Current	$\frac{PTIC(I)}{PTIC(x)}$
FM,ICPS	0.10s 30	$\tau_{\|I\|} = 0.10s$	1
FM,PRBS	0.10s 30	$min_\tau = 0.05s$	1

Equation	Description
$\tau(vco)$	Time constant for VCO
$\frac{PTIC(I)}{PTIC(x)}$	How many PTIC(I) utilized each PTIC(x)
min_τ	Minimum clock period in PRBS
$\tau_{\|I\|}$	Amplitude Period in ICPS

The Figure 2 shows three computed experiments. These training pattern exhibit fixed amplitude for displacement and persitent signals in frequency.

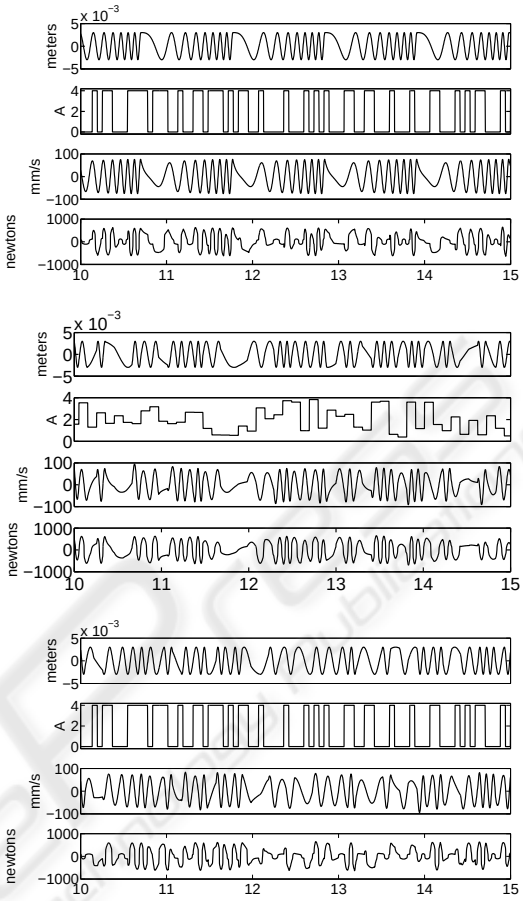

Figure 2: Experimental training patterns. Top plot shows a (*CHS,PRBS*). Middle plot shows a (*FM,ICPS*). Bottom plot describes a (*FM,PRBS*).

4 RESULTS

Performing an analysis of the models (1) and (2) and a-priori knowledge of *MR* damper dynamics, the modified models and its degree of freedoms were proposed. The *D*egree *o*f *F*reedom (*DoF*) of the model represents a main variation in the original structure of the model

Then, for the given experimental data sets, the two *MR* damper models were trained. The first trained model was the modified version of (1). The new model has added regressors of the current. Each delayed value of current is raised to power two. Thus, the augmented regressors structure were:

$$a_{10} \cdot I_{k-1}^2 + \cdots + a_{\{10+d-1\}} \cdot I_{k-(1+d)}^2 \qquad (3)$$

The resultant model could have from 11 to 14 parameters, then its *DoF* is the number of parameters for *I*. The second trained model was the modified SP model (4). The modification consisted of the incorporation of the factor I^{q_j} as direct input on both terms, where j=$\{1,2\}$ is the j-esime model term. The *DoF*s of model (4) were the power q_j, where its possible values were $\{0.5, 0.33, 0.25, 0.2\}$. The parameters number remains the same.

$$f_{MR} = a_1 \cdot I^{q_1} tanh\left(a_3\left(\dot{x} + \frac{a_4}{a_5}x\right)\right) + a_2 \cdot I^{q_2}\left(\dot{x} + \frac{a_4}{a_5}x\right) \qquad (4)$$

Finally, the modified models were identified by nonlinear curve fitting using the non-linear least squares algorithm. Based on these models, the DoEs were validated.

The training patterns have persistent signals with richness frequency content for each signal (x, $\dot{x}$, I, f_{MR}). For each experiment, the model was fitted at each defined *DoF*. Then a validation of the model via ESR was performed with the rest of the experiments and the ESR average was computed.

This process was repeated until all the possible values of *DoF* were varied and the resultant model

was fitted.

After obtaining all the fit measures per DoF for experiment data sets, a sort process from lowest to highest ESR was done. This step did include all the experiments. The combination of *DoF* and experiment with the lowest error-to-noise ratio was selected as the best.

Identification and validation were performed for all the experiments and models. Therefore proposed NARX model was submitted to the variation in number of coefficients. The semi-phenomenological model always maintained five coefficients along *DoF* variations. The models include the electric current as natural input. The validation process confirmed that the emulation of bi-viscous and hysteretic features by the proposed models are dependent on the design of experiments.

Table 4: Comparison of ESR results for different training patterns. M is the type of model. E is the number of training pattern, ESR AVG is the average ESR. BEST ESR is the best obtained ESR.

M	E	ESR AVG	BEST ESR
BB	8	0.002	0.0009
	9	0.003	0.0009
	5	0.0011	0.0010
	11	2139	2232
	6	2.0582	3.6940
	7	1.1010	1.9761
SP	8	0.0239	0.0212
	1	0.0235	0.0202
	4	0.0240	0.0205
	10	0.1916	0.1055
	3	0.1002	0.1094
	11	0.2132	0.0979

In Table 4, general approach results are shown. BB and SP correspond to the modified model (1) and the model (4) respectively. E column sorts the experiments by the top 3 performance and the worst 3 for the same DoF. The next columns ESR AVG and SD shows the overall ESR statistical behavior, in other words, for all DoF variations and for all validations with a specific experiment. For example, the first row specifies that EXP 8 for NARX proposed model has an average $ESR = 0.0002$ when the coefficients obtained by experiment 8 are used to validate others patterns. For this row, the best model has a $DoF = 2$. An analysis of the full table demonstrates that the best performing E is the number 8 because it has the lowest ESR values. For completeness, the values for DoFs have been included into the Table 4. The best performing *DoF* were: number of regressors of electric current equal to 2 for NARX model and $q_1 = 0.5, q_2 = 0.2$ for electric current dependent semi-phenomenological model.

By other side, the experiments 11, 6 and 7 used to fit BB and the experiments 10, 3 and 11 used to fit SP have big ESRs (i. e. lack of fit). The experiment 11 is repeated for both worst cases, hence the use of road profiles could generate skewed models. Thus, the configuration of input patters has high signification on the learning of model parameters.

Based on the results, a frequency modulated displacement, with the same spectral frequency content as road profile and an electrical current excitation with ICPS shaping can recreate the dynamical force response of *MR* Damper devices, regardless of the *MR* damper model's structure.

Moreover, coefficients are robust when model is tested with other patterns (cross validation), obtaining lows ESRs. The ESR span intervals were for NARXs $(6.17x10^{-5}, 0.00026)$, for SP $(0.00635, 0.05687)$ and for P $(0.02234, 0.06917)$, respectively. The experiments 5, 7, 9 y 12 (current equal to PRBS) for modified SP always offer an $ESR \geq 0.15$ which means that discontinuous values of current are not proper for model.

4.1 Discussion

The classic DoE has poor frequency content in electric current and excessive repetitions in displacement. Hence, the number of experiments are a multiple of the values of the tested electric current plus the replicates for each experiment. The lengths of time of the eleven DoEs in this work were between 30-60 seconds. The maximum number of experiments will be 30, including the replicates. The realistic nature of exogenous and actuation variables allows a safe test.

The best learning of the coefficients in each tested model was successfully with the training pattern *FM+ICPS*. The frequency modulated displacement implies a continuous changes of slope implying the persistence of the effect of the velocity over *MR* damper. Therefore, with a short and continuous test, the uniform coverage of the semi-active zone, (the exploration of energy and power capabilities) in *MR* damper is achieved.

5 CONCLUSIONS

A comparative analysis of training pattern for identification of *MR* damper models was done. Two models were exploited to validate the proposal: non-linear ARX and Semi-phenomenological models. The key

variables in training patterns are the frequency bandwidth and the electric current.

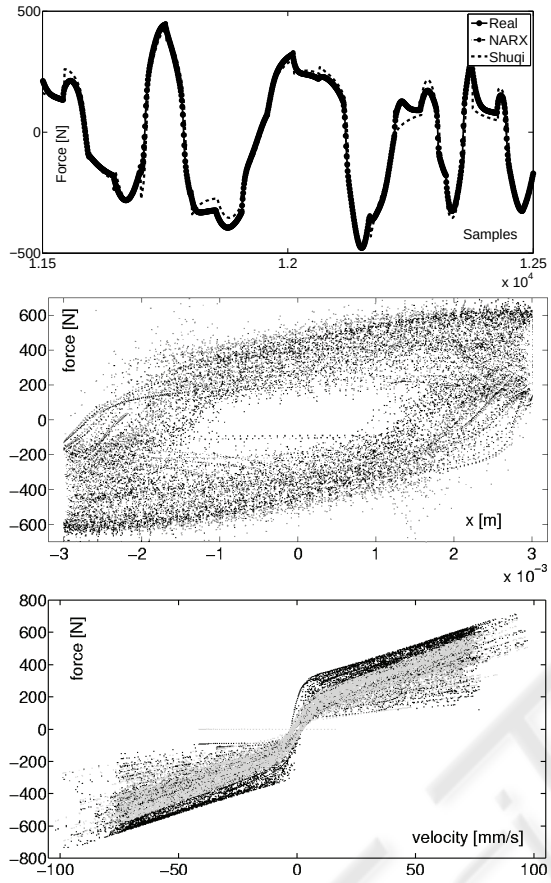

Figure 3: Top plot. Comparison of simulated responses versus experiment 8. Middle and bottom plots show the power and energy extraction using the experiment 8. The black dots are experimental data. The gray dots are emulated data by SP proposed model with a $q_1 = 0.5$, $q_2 = 0.2$.

I was validated that the configuration of the training patterns has a high impact over the model fitting. Features as short duration, continuity, uniform coverage of electric current and displacement ranges are needed. Also, the use of the model must be considered into the DoE.

REFERENCES

Burton, S., Makris, N., Konstantopoulos, I., and Antsaklis, P. (1996). Modeling the Response of ER Damper: Phenomenology and Emulation. *Eng. Mech.*, 122:897–906.

Chang, C. and Zhou, L. (2002). Neural Network Emulation of Inverse Dynamics for a MR Damper. *Struct. Eng.*, 128:231–239.

Du, H., Lam, J., and Zhang, N. (2006). Modelling of a Magneto-Rheological Damper by Evolving Radial Basis Function Networks. *Eng. Apps. of Art. Intell.*, 19(8):869–881.

Guo, S., Yang, S., and Pan, C. (2006). Dynamical Modeling of Magneto-rheological Damper Behaviors. *Int. Mater, Sys. and Struct.*, 17:3–14.

Li, W. H., Yao, G. Z., and Chen, G. (2000). Testing and Steady State Modeling of a Linear MR Damper under Sinusoidal Loading. *Smart Materials Structures*, 9:95–102.

Lozoya-Santos, J. J., Morales-Menendez, R., and Ramirez-Mendoza, R. (2009). Design of Experiments for MR Damper Modelling. To appear in *Neural Netwotks, Int. Joint Conf. on, IEEE Proc.*

Nino-Juarez, E., Morales-Menendez, R., Ramirez-Mendoza, R., and Dugard, L. (2008). Minimizing the Frequency in a Black Box Model of a MR Damper. In *11th Mini Conf on Vehicle Sys. Dyn., Ident. and Anomalies*.

Savaresi, S. M., Bittanti, S., and Montiglio, M. (2005). Identification of Semi-Physical and Black-Box Non-Linear Models: the Case of MR-Dampers for Vehicles Control. *Automatica,*, 41(1):113–127.

Shivaram, A. C. and Gangadharan, K. V. (2007). Statistical Modeling of a MR Fluid Damper using the Design of Experiments Approach. *Smart Mater. and Struct.*, 16(4):1310–1314.

Spencer, B., Dyke, S., Sain, M., and Carlson, J. (1996). Phenomenological Model of a MR Damper. *ASCE J of Eng Mechanics*.

Wang, D.-H. and Liao, W.-H. (2001). Neural Network Modeling and Controllers for Magneto-Rheological Fluid Dampers. In *Fuzzy Sys.. The 10th IEEE Int. Conf. on*, volume 3, pages 1323–1326.

Wang, D. H. and Liao, W. H. (2005). Modeling and Control of Magnetorheological Fluid Dampers using Neural Networks. *Smart Mater. Struct.*, 14:111–126.

Wang, L. X. and Kamath, H. (2006). Modelling Hysteretic Behaviour in MR Fluids and Dampers using Phase-Transition Theory. *Smart Mater. Struct.*, 15:1725–1733.